

Melting and solidification: processes and models/Experiments for solidification benchmarks

Modeling fragmentation of plasma-sprayed particles impacting on a solid surface at room temperature

André McDonald^{a,*}, Michelle Xue^a, Sanjeev Chandra^a, Javad Mostaghimi^a,
Christian Moreau^b

^a Center for Advanced Coating Technology, Department of Mechanical and Industrial Engineering, University of Toronto, Toronto, Ontario, M5S 1A4 Canada

^b National Research Council Canada, Industrial Materials Institute, Boucherville, Québec, J4B 6Y4 Canada

Available online 21 June 2007

Abstract

Molybdenum particles were melted and accelerated by a plasma jet to impact on glass surfaces held at room temperature. A fast charge-coupled device (CCD) camera was triggered to capture images of the particles during spreading. Splats on the glass held at ambient temperature fragmented, leaving only a solidified central core. A 3D model of droplet impact and solidification was used to simulate the impact and spreading of these plasma-sprayed particles. The thermal contact resistance, which was estimated from an existing heat conduction model, was used as an input parameter in the 3D model. It was found that the thermal contact resistance between the splat central core and the glass was two orders of magnitude lower than that between the rest of the splat fluid and the surface. This suggests that the physical contact between the fluid in the splat central core and the glass surface can be improved by the large pressure generated during impact. **To cite this article:** A. McDonald et al., *C. R. Mecanique 335 (2007)*.

© 2007 Académie des sciences. Published by Elsevier Masson SAS. All rights reserved.

Résumé

Modélisation de la fragmentation de particules projetées par plasma sur des surfaces solides à température ambiante. Des particules de molybdène sont fondues et accélérées par un jet de plasma et sont projetées à haute vitesse sur des surfaces de verre à température ambiante. Une caméra rapide à dispositif à transfert de charge (CCD) est déclenchée pour photographier les particules lors de leur écrasement. Sur le verre maintenu à température ambiante, les gouttelettes écrasées se fragmentent en périphérie laissant la partie centrale intacte. Un modèle numérique 3D est utilisé pour simuler l'impact et l'étalement des particules projetées par plasma. La résistance thermique de contact qui est estimée à partir d'un modèle de conduction de chaleur, est un paramètre d'entrée du modèle numérique 3D. Nous avons trouvé que la résistance thermique de contact entre la région centrale de la gouttelette et le verre était deux ordres de grandeur plus basse que celle entre la périphérie et le verre. Ceci suggère que le contact physique entre le fluide de la partie centrale de la gouttelette et la surface de verre est amélioré par la pression élevée lors de l'impact. **Pour citer cet article :** A. McDonald et al., *C. R. Mecanique 335 (2007)*.

© 2007 Académie des sciences. Published by Elsevier Masson SAS. All rights reserved.

Keywords: Fluid mechanics; Cooling rate; Particle impact; Splat fragmentation; Thermal contact resistance

Mots-clés : Mécanique des fluides ; Vitesse de refroidissement ; Impact de particules ; Fragmentation de gouttelettes ; Résistance thermique de contact

* Corresponding author.

E-mail address: mcdonald@mie.utoronto.ca (A. McDonald).

1. Introduction

Fragmentation and splashing of molten particles impacting on a solid surface are influenced by many factors. When water droplets impinge on stainless steel surfaces, the impact velocity is the main factor that promotes splashing [1]. However, when a molten metal droplet lands on a colder surface, solidification and heat transfer play a major role during particle fragmentation, and changes in thermal contact resistance at the droplet-substrate interface can affect the shape of the solidified splat. Application of an organic compound to the substrate surface has been found to increase the incidence of splashing [2]. Heating the coated substrate 50 °C above the boiling point of the organic covering eliminated splashing and produced disk-like splats. Jiang et al. [3] found that removal of surface adsorbates and condensates reduced splashing. It was proposed that on non-heated surfaces, these contaminants vaporize and form a gas barrier beneath the splat, restricting splat solidification and promoting fragmentation of the liquid film.

Splat fragmentation and splashing observed on non-heated substrates have been attributed to the large thermal contact resistance between the substrate and splat [4–6]. Bianchi et al. [4] used a 1D numerical model to estimate the thermal contact resistance between plasma-sprayed zirconia and stainless steel. It was found that thermal contact resistance on a non-heated surface may be one to three orders of magnitude larger than that on a heated surface. More precise values were obtained by using the splat cooling rates in a one-dimensional heat conduction model [6]. It was shown that the thermal contact resistance between molybdenum splats and heated Inconel 625 was an order of magnitude smaller than that between the splats and non-heated Inconel 625 [6].

Numerical models have been used to predict the experimentally observed disintegration and splashing patterns during droplet spreading. Zhang et al. [7] used a two-dimensional numerical model based on the volume-of-fluid (VOF) scheme to simulate the splashing of plasma-sprayed molybdenum on steel substrates. It was found that as the splat melted the substrate during spreading, the molybdenum/steel liquid mixture jetted out at the edge of the unmolten substrate. Li et al. [8] extended the work of Zhang et al. [7] to show that substrate melting promoted fragmentation of the splat, producing a flower-like morphology. In-situ photographs of plasma-sprayed molybdenum spreading on glass held at room temperature have shown significant splat fragmentation [9]. However, few numerical models have been developed to simulate this type of splat spreading and fragmentation.

The objectives of this study were to: (i) photograph the fragmentation of plasma-sprayed molybdenum particles that impacted glass held at room temperature; (ii) use a 3D model of droplet impact and solidification to simulate the impact, spreading, and fragmentation of these particles; and (iii) compare numerical simulation results with experimental observations.

2. Experimental method

The experimental assembly and method used to capture in-situ images of the spreading splats have been described in detail by McDonald et al. [9]. A SG100 plasma torch (Praxair Surface Technologies, Indianapolis, IN) was used to melt and accelerate the dense, spherical molybdenum powder particles (SD152, Osram Sylvania Chemical and Metallurgical Products, Towanda, PA), sieved to diameters between 38 and 60 μm . The substrate was a glass microscope slide (Fisher Scientific, Pittsburgh, PA) that was washed with water and ethanol and dried in an oven at 140 °C for 30 minutes.

To illuminate the impacting particles, a 5 ± 2 ns duration pulse of light from a Nd:YAG laser (Continuum Minilite, Santa Clara, CA) was used. A 12-bit CCD camera (QImaging, Burnaby, BC) was used to capture single images of the spreading particles from behind the glass substrate. The camera was connected to a long-range microscope (Astro-optics Division, Montpelier, MD) that had an 80% neutral density (ND) filter to attenuate the intensity of the laser beam. By varying the instant at which the laser was pulsed, different stages of particle impact and spread were photographed. The images captured by the camera were digitized by a frame grabber and recorded on a personal computer.

3. Numerical method

The three-dimensional numerical model of droplet impact used in this study solves the equations of mass, momentum, and energy conservation. Pasandideh-Fard et al. [10] provide detailed descriptions of the model.

The free surface of the droplet was modeled by defining the volume-of-fluid scalar (f) as the fraction of the cell volume occupied by fluid. If this scalar was equal to one, the cell was completely filled with fluid; if it was zero, the cell was empty; and if the fraction was between zero and one, the cell contained a free surface. To identify and track the solid phase, a second liquid volume fraction, λ was introduced. If this parameter was equal to one, the material was in the liquid phase and it was zero when the material was in the solid phase. When both liquid and solid phases were present, the liquid phase was assumed to have volume fraction, λ and the solid phase, $1 - \lambda$. The advection equation of the volume-of-fluid scalar, which accounts for solidification, is:

$$\frac{\partial f}{\partial t} + (\lambda \vec{u} \cdot \vec{\nabla}) f = 0 \quad (1)$$

where \vec{u} represents the velocity vector and t , the time.

After defining the new volume fraction for the solid cells, the conservation equations of mass and momentum were written as:

$$\vec{\nabla} \cdot (\lambda \vec{u}) = 0 \quad (2)$$

$$\frac{\partial (\lambda \vec{u})}{\partial t} + (\lambda \vec{u} \cdot \vec{\nabla}) \vec{u} = \frac{-\lambda}{\rho} \vec{\nabla} p + \lambda \nu \nabla^2 \vec{u} + \frac{\lambda}{\rho} \vec{F}_b \quad (3)$$

where p represents the pressure, ρ the density, ν the kinematic viscosity, and \vec{F}_b body forces acting on the fluid. The energy equation was given as:

$$\rho \frac{\partial h}{\partial t} + \rho (\vec{u} \cdot \vec{\nabla}) h = \nabla^2 (\beta h) + \nabla^2 \phi \quad (4)$$

where h is the enthalpy and β is the enthalpy coefficient [10].

No-slip and no-penetration boundary conditions were applied at the solid substrate surface. The effect of convection and radiation from the free liquid surface was neglected. Free surfaces of the droplets and exposed portions of the substrate were assumed to be adiabatic. Mostaghimi et al. [11] have shown that heat loss by convection at the free surfaces was three orders of magnitude lower than conduction at the droplet-substrate interface. Therefore, the adiabatic condition at the free surface was reasonable.

The governing equations were discretized by using a finite volume technique on a three-dimensional Eulerian structured grid [10]. In order to save computational time and to reduce the domain size, only one-quarter of the droplet and splat was modeled. The numerical computations were performed on an AMD Athlon 64, 3400 PC. The average CPU time was 24 hours.

4. Results and discussion

McDonald et al. [9] have shown images of the spreading and fragmentation of plasma-sprayed molybdenum particles on a glass slide held either at room temperature or at 400 °C. On non-heated glass, the particles spread into a thin sheet and disintegrate, initially from the solidified central core and then from sites within the sheet. Disintegration from within the thin sheet occurred through the formation of holes, which grew until only the solidified central core remained attached to the surface. On glass held at 400 °C, disintegration was significantly reduced and a small, disk-like splat remained on the surface. It was shown that on heated glass, the entire splat area was in good physical contact with the substrate, while on glass held at room temperature, only the splat central core area was in contact with the glass.

It was suggested that a gas barrier separated the splat from the non-heated glass, reducing contact. This gas barrier increased the thermal contact resistance between the splat and the substrate, reducing the splat cooling rate and permitting the splat to remain as a liquid longer. On non-heated glass, the average cooling rate was $3.3 \pm 0.2 \times 10^7$ K/s, and on heated glass, it was almost an order of magnitude larger at $22 \pm 1.2 \times 10^7$ K/s [9]. These cooling rates, the physical properties of molybdenum and glass [9], and a one-dimensional heat conduction model [6] were used to estimate the thermal contact resistance between the splat and substrate. McDonald et al. [6] showed the detailed derivation of the heat conduction model. The average thermal contact resistance between molybdenum splats and glass held at room temperature was $5.0 \pm 0.5 \times 10^{-5}$ m² K/W, while between the splats and glass heated to 400 °C, it was $6.5 \pm 1.0 \times 10^{-7}$ m² K/W. These thermal contact resistance estimates represent the average values over the

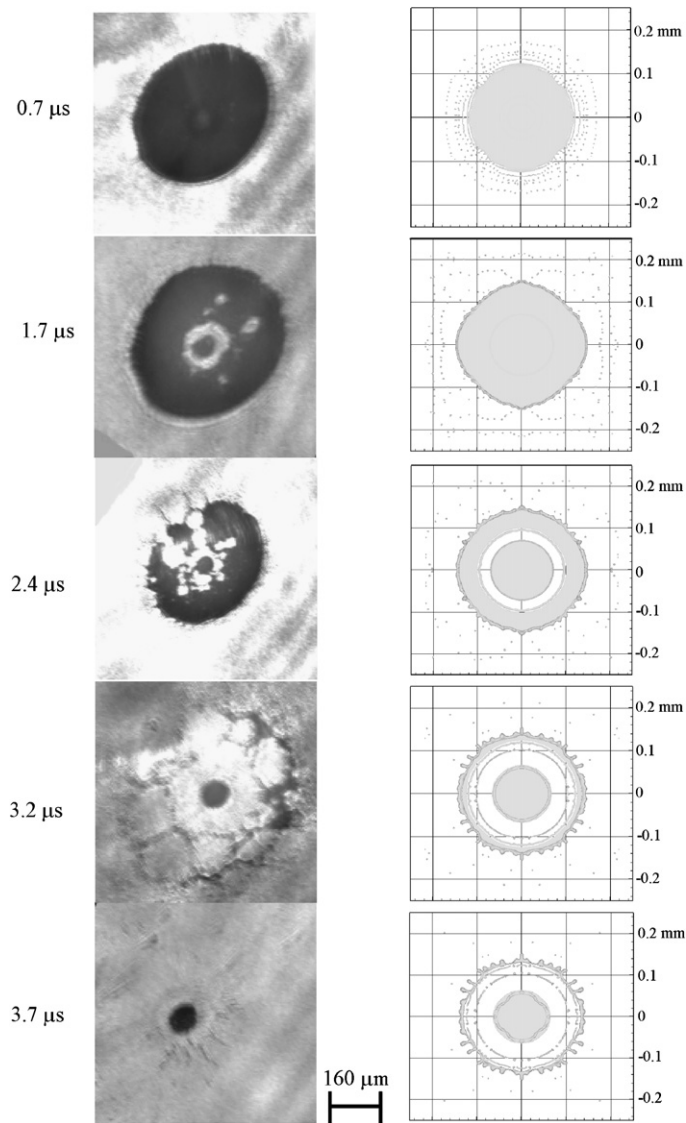


Fig. 1. (a) Experimental photographs and (b) numerical simulation images of molybdenum particles spreading on non-heated glass.

Fig. 1. (a) Photos expérimentales et (b) images correspondantes calculées à l'aide du modèle numérique de particules de molybdène lors de leur étalement sur le verre froid.

entire area of the splat and during the spreading process. Since it has been shown that splats on heated glass and the central core of the splats on non-heated glass make good physical contact with the substrate due to the large impact pressure [9], it was assumed that the thermal contact resistance was the same order of magnitude ($10^{-7} \text{ m}^2 \text{ K/W}$). The rest of the splat on the non-heated glass, outside of the central core, had a higher thermal contact resistance on the order of $10^{-5} \text{ m}^2 \text{ K/W}$.

The spatially varying thermal contact resistance between the molybdenum splat and glass held at room temperature was used as an input parameter into a 3D numerical model. Fig. 1 shows the images generated by the numerical model for a particle with a 50 μm diameter, in-flight temperature of 2950 °C , and impact velocity of 130 m/s . The figure also shows photographs of different splats captured at specific times after impact. A thermal contact resistance of $1.0 \times 10^{-7} \text{ m}^2 \text{ K/W}$ was specified for the splat central core in contact with the glass. The diameter of the central core was measured from images of the splat after spreading, fragmentation, and solidification. Under the rest of the

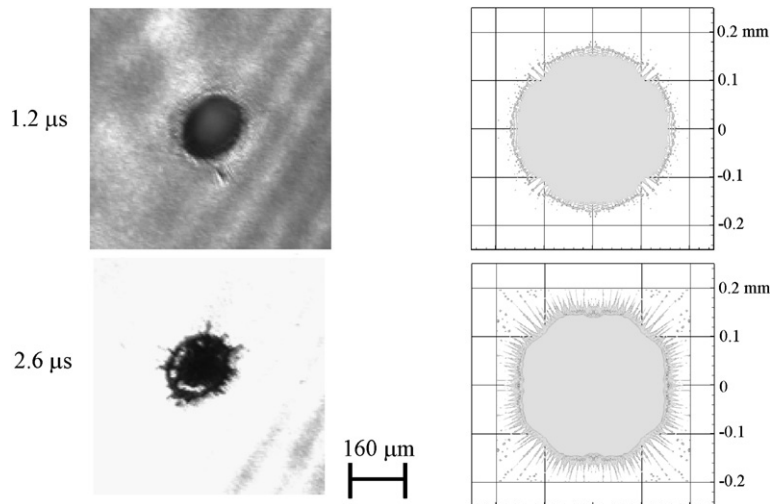


Fig. 2. (a) Experimental photographs and (b) numerical simulation images of molybdenum particles spreading on glass at 400 °C.

Fig. 2. (a) Photos expérimentales et (b) images correspondantes calculées à l'aide du modèle numérique de particules de molybdène lors de leur étalement sur le verre à 400 °C.

splat, a thermal contact resistance of $5.0 \times 10^{-5} \text{ m}^2 \text{ K/W}$ was specified, based on the result of the 1D heat conduction model [6] for this particle.

The results from the numerical simulation (Fig. 1(b)) show that as the splat spreads, it fragments from the solidified central core. Since the thermal contact resistance in the central core is small ($1.0 \times 10^{-7} \text{ m}^2 \text{ K/W}$) compared to the rest of the splat, it solidified faster. The rest of the splat, in liquid form, continues to spread and disintegrate, until only the central core remained attached to the surface, surrounded by solidified debris.

The disintegration pattern of large holes in the thin sheet of the splat was not captured exactly by the numerical simulation. Dombrowski and Fraser [12] have suggested that disruptions in thin sheets of high viscosity materials, such as molybdenum, are caused by the presence of unwettable particles. Modelling such disruptions can be challenging, since they will occur at random locations in the thin sheet of the splat where impurities or solidified regions may be present. In simulations, where circular symmetry exists, film ruptures also occur in a symmetric fashion.

Fig. 2 shows experimental and simulated images of a plasma-sprayed molybdenum particle with a 60 μm diameter, in-flight temperature of 2950 °C, and impact velocity of 120 m/s on glass heated to 400 °C. Based on the heat conduction model [6], the thermal contact resistance between the splat and the heated glass was $2.5 \times 10^{-7} \text{ m}^2 \text{ K/W}$. The images of Fig. 2 also show the splat, 2.6 μs after impact, when spreading and solidification were completed. On heated glass, the splat cooling rate was high and the thermal contact resistance between the splat and surface was low, promoting faster solidification on this surface. There was splashing and formation of fingers at the splat periphery, possibly induced by the solid portions of the splat that acted as impediments to flow during spreading. This type of disruption is significantly different from that observed on non-heated glass where disruption occurs due to the formation of holes in the thin liquid sheet of the splat. On glass held at 400 °C, the results of the numerical model agree well with the experimental images. Since the splat is in good contact with the glass, a no-slip boundary condition exists at the splat-glass interface. The single-fluid numerical model used in this study is well suited to simulate the splat spreading, solidification, and splashing on the heated surface.

Fig. 1(a) shows that after 2 μs after impact, the observed splat diameter is approximately 500 μm , while the simulation (Fig. 1(b)) predicts diameters of about 300 μm . The presence of a possible gas barrier between the splat and non-heated glass will invoke a slip boundary condition at the splat-substrate interface. The slip boundary condition at the interface will influence the diameter of the splat predicted by the numerical model. Since the model assumes a no-slip boundary condition, viscous dissipation losses will be greater, reducing the splat diameter [9]. A two-fluid numerical model, capable of simulating the gas barrier, may predict better the observed splat diameters. On the heated glass, there is a no-slip boundary condition at the splat-glass interface [9]. Fig. 2(a) shows that the splat diameter is approximately 220 μm , while the numerical model predicts a diameter of 300 μm (Fig. 2(b)). These results confirm

observations by Jiang et al. [3] that there exists a condensate/adsorbate gas barrier between the splat and non-heated glass.

5. Conclusion

In-situ photographs showing the spreading, fragmentation, and splashing of plasma-sprayed molybdenum on glass held at room temperature and at 400 °C were shown. A 3D numerical model of droplet impact and solidification was used to simulate the spreading and fragmentation of these particles. On non-heated glass, a spatially varying thermal contact resistance was applied between the splat and the glass. It was found that in the central core of the splat, the thermal contact resistance was two orders of magnitude smaller than under the rest of the splat. This reduced cooling in the splat periphery, promoting fragmentation of the thin liquid sheet. The central core solidified and remained attached to the surface.

Comparing computer generated images with experimental photographs supported the hypothesis of a gas barrier and a slip boundary condition at the interface of the splat and non-heated glass. The numerical model assumed a no-slip boundary condition at the splat-glass interface, resulting in splat diameters that were more than 40% smaller than that observed in experiments. On heated glass, where a no-slip boundary condition exists at the interface, the difference in diameter was significantly smaller. A two-fluid numerical model, capable of modelling the gas barrier, may be better suited to simulate spreading and slipping on non-heated surfaces.

References

- [1] N. Mehdizadeh, S. Chandra, J. Mostaghimi, Formation of fingers around the edges of a drop hitting a metal plate with high velocity, *J. Fluid Mech.* 510 (2004) 353–373.
- [2] C. Li, J. Li, W. Wong, The effect of substrate preheating and surface organic covering on splat formation, in: C. Coddet (Ed.), *Thermal Spray: Meeting the Challenges of the 21st Century*, May 25–29, 1998 (Nice, France), ASM International, 1998, pp. 473–480.
- [3] X. Jiang, Y. Wan, H. Hermann, S. Sampath, Role of condensates and adsorbates on substrate surface on fragmentation of impinging molten droplets during thermal spray, *Thin Solid Films* 385 (2001) 132–141.
- [4] L. Bianchi, A. Leger, M. Vardelle, A. Vardelle, P. Fauchais, Splat formation and cooling of plasma-sprayed zirconia, *Thin Solid Films* 305 (1997) 35–47.
- [5] C. Moreau, P. Cielo, M. Lamontagne, S. Dallaire, M. Vardelle, Impacting particle temperature monitoring during plasma spray deposition, *Meas. Sci. Technol.* 1 (1990) 807–814.
- [6] A. McDonald, C. Moreau, S. Chandra, Thermal contact resistance between plasma-sprayed particles and flat surfaces, *Int. J. Heat Mass Transfer* 50 (2007) 1737–1749.
- [7] H. Zhang, X. Wang, L. Zheng, X. Jiang, Studies of splat morphology and rapid solidification during thermal spraying, *Int. J. Heat Mass Transfer* 44 (2001) 4579–4592.
- [8] L. Li, X. Wang, G. Wei, A. Vaidya, H. Zhang, S. Sampath, Substrate melting during thermal spray splat quenching, *Thin Solid Films* 468 (2004) 113–119.
- [9] A. McDonald, M. Lamontagne, C. Moreau, S. Chandra, Impact of plasma-sprayed metal particles on hot and cold glass surfaces, *Thin Solid Films* 514 (2006) 212–222.
- [10] M. Pasandideh-Fard, S. Chandra, J. Mostaghimi, A three-dimensional model of droplet impact and solidification, *Int. J. Heat Mass Transfer* 45 (2002) 2229–2242.
- [11] J. Mostaghimi, M. Pasandideh-Fard, S. Chandra, Dynamics of splat formation in plasma spray coating process, *Plasma Chem. Plasma Process.* 22 (2002) 59–84.
- [12] N. Dombrowski, R. Fraser, A photographic investigation into the disintegration of liquid sheets, *Trans. Royal Soc. London A* 247 (1954) 101–130.